Correlation of Magnetic Susceptibility and R2* with iron in ferritin

Weili Zheng[1], Yu-Chung Norman Cheng[1], Saifeng Liu[2], Helen Nichol[3], and E. Mark Haacke[1]

[1]Radiology, Wayne State University, Detroit, MI, United States, [2]School of Biomedical Engineering, McMaster University, Hamilton, Ontario, Canada, [3]Department of Anatomy and Cell Biology, University of Saskatchewan, Saskatoon, Saskatchewan, Canada

Introduction. Iron is an important endogenous biomarker for many neurological diseases as well as for normal aging. However, correlating iron with susceptibility mapping has proven to be a challenging problem. Values from the literature vary largely (1-3) when different background removal and susceptibility mapping methods are used. Since most of the iron in the brain is stored in ferritin as a paramagnetic iron oxide (4), an iron-loaded ferritin phantom was used here to investigate the correlation of iron with susceptibility and the other commonly used iron predictor, R2* (1/T2*).

Methods. Horse spleen ferritin (Ref. F4503, *Sigma-Aldrich*.) was serially diluted in warm gelatin. Ferritin phantoms were prepared for MRI by aspirating this solution into straws embedded in the same concentration of gelatin in cylindrical containers. Empty straw phantoms were also made to validate the background removal and susceptibility mapping methods against the known air-gelatin susceptibility.

The same dilutions were stored in small airtight containers and transported to the Stanford Synchrotron Radiation Lightsource for Rapid Scanning X-Ray Florescence (RS-XRF) imaging on beamline 10-2 using the setup described by Hopp et al (4). Fluorescent energy windows were centered for Fe (6.21 - 6.70 keV), scatter and total incoming counts. Sam's Microanalysis kit software (http://ssrl.slac.stanford.edu/~swebb/smak.html) was used to normalize the raw data to incoming counts and to calculate iron concentrations by comparison to an iron XRF standard (Micromatters).

MR raw data were collected on a 3T Siemens Verio system using a T2* weighted multi-echo SWI sequence (5) with 11 echoes (TR=40ms, FA=15°). The resolution was 1mm×1mm×1mm with matrix of 256×256×128. The shortest echo time was 6.37ms with a 2.51ms increment for the other 10 echoes. The magnitude and phase images were reconstructed from raw data for each channel and combined. T2* maps were reconstructed from the magnitude images. Geometry of the ferritin samples were segmented from multi-echo spin echo images (TR=2000ms, resolution 0.22mm×0.22mm×3mm) and registered to phase images.

The phase images were unwrapped using Prelude in FLS. The background inside the dipole regions were extrapolated from the background outside, then phase dipole was subtracted. The susceptibility of ferritin straws was estimated using the forward approach (6). All the steps (Fig.1) were calculated in MATLAB codes.

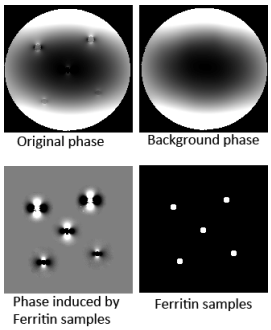

Fig.1. Removing the background and subtract the phase dipoles.

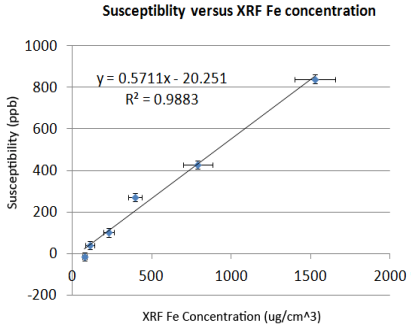

Fig.2. Correlation between susceptibility and ferritin iron concentration

Results. Our results showed that the average air-gelatin susceptibility was 9.4592±0.0042ppb. This means the background removal and susceptibility calculation used here was reliable as applied to the ferritin iron samples.

We determined that susceptibility change per microgram of iron (as determined with XRF) in a gram of tissue was 0.57±0.1 ppb (see Fig. 2). Table 1 compares our results with previous correlations obtained from in vivo human data at 3T and 7T using the non-heme iron estimation equation developed by Hallgren and Sourander (7). Since our result is close to that obtained in vivo by Shmueli et al. (1) and Wharton et al. (2), ferritin phantoms model human brain iron susceptibility quite well. When there was 77 µg Fe/ml in the lowest concentration ferritin sample, the phase dipole changed the sign and the susceptibility was found as -14ppb. This negative susceptibility in the presence of iron and the difference between our results and the theoretical value (8) indicate chemical exchange (9) may contribute to susceptibility change and not negligible. The difference among published results shows that correction of myelin made much more difference than the variation caused by different mapping methods.

Table1. Published correlations between susceptibility and iron concentration

	Authors	Slope	Field	Sample	Iron conc.
No myelin	Our result	0.57	3T	Ferritin	XRF
Myelin not corrected	Shmueli et al. (1)	0.56	7T	in vivo	(7)
	Wharton et al. (2)	0.75	7T	in vivo	(7)
Myelin corrected	Schweser et al. (3)	1.3	3T	in vivo	(7)
Theoretical	Schenck et al. (8)	1.27			

Table2. Published correlations between R* and iron concentration

Authors	Slope	Field	Sample	Iron conc.
Our result	0.0098X+1.21	3T	Ferritin	XRF
Shmueli et al. (1)	0.21x + 28.76	3T	in vivo	(7)
Yao et al. (10)	0.048X+1.42	7T	in vivo	(7)
Yao et al. (10)	0.0099X+Y	7T	Dry tissue	ICPMS
Yao et al. (10)	0.12X+Y	3T	in vivo	(7)
Langkammer et al. (11)	0.27X+14.3	3T	ex vivo	ICPMS

We also found that R2* correlated with iron concentration ($R2^*(HZ)=0.0098*C_{iron}$(µg Fe/g wet tissue)+1.2116, R^2=0.9953). Our results are compared with previous published results in Table 2. R2* varies not only with the field strength but also with the tissue composition and chemical environment. This is because R2*=R2+R2' and R2' is sensitive to many other factors besides iron content and changes from ferritin gelatin to tissue and from tissue to tissue (12). The big difference between our ferritin R2* results and in vivo results indicates ferritin in gelatin phantoms cannot be used to reliably estimate human brain iron using R2*.

Conclusion. Susceptibility mapping predicts iron more reliably than does R2*. Ferritin gelatin phantoms may are a feasible model for human brain iron susceptibility studies. The effect of myelin and chemical exchange may not be negligible when predicting iron using susceptibility mapping and this needs to be further explored in order to accurately predict ferritin iron concentrations in vivo.

Acknowledgments. This work is supported by Heart and Stroke Foundation of Canada (HSFC) and the Canadian Institutes of Health Research (CIHR) - Institute of Circulatory and Respiratory Health, Clinical Imaging Initiative (FRN - 99472) to HN. The authors would like to thank Sam Webb at the Stanford Synchrotron Radiation Lightsource for his help in collecting XRF data. The authors would also like to thank Dr. Karin Shmueli at NINDS, NIH for her valuable discussions of the literature.

References: (1) Shmueli et al. MRM, 62:1510, 2009. (2) Wharton et al. NeuroImage, 53:515, 2010. (3) Schweser et al. NeuroImage, 54:2789, 2011. (4) Hopp et al. JMRI, 31:1346, 2010. (5) Haacke et al. AJNR, 30:19, 2009. (6) Li, MRM, 46: 907, 2001. (7) Hallgrena and Sourander, J. Neurochem. 3 (1): 41, 1958. (8). Schenck, Ann. NY Acad. Aci. 649: 285, 1992. (9) Shmueli et al. MRM, 65: 35, 2011. (10) Yao et al. NeuroImage, 44:1259, 2009. (11) Langkammer et al. Radiology, 257: 455, 2010. (12) Gossuin et al. JMRI, 20 (4):690, 2004.